



Special Feature: Applied Nanoscale Morphology

Research Report

Optical Filters Using Metal-based Metamaterial

Daisuke Inoue, Atsushi Miura, Tsuyoshi Nomura, Hisayoshi Fujikawa, Kazuo Sato, Naoki Ikeda, Daiju Tsuya, Yoshimasa Sugimoto and Yasuo Koide

Report received on Mar. 19, 2014

■ABSTRACT■ Since it was first discovered that enhanced optical transmission can occur through periodic arrays of holes with sub-wavelength dimensions formed in optically-thick metallic films, many potential applications have been conceived. These include, for example, wavelength filters, light extraction from light emitting diodes, and sub-wavelength photolithography. In the present study, this phenomenon was utilized to fabricate color filters consisting of periodic arrays of sub-wavelength holes and slits in aluminum films. The optical properties of the different metamaterials were experimentally evaluated, and the results were compared to those obtained from calculations using the finite difference time domain method. In the case of a hexagonal array of circular nanoholes, the transmittance showed no dependence on the polarization direction of the incident light. Thus, by suitable choice of the hole size and the lattice periodicity, these metamaterials could be made to act as polarization-independent red-green-blue color filters. In contrast, for an aluminum film containing a nanoslit pattern, the transmittance was strongly polarization dependent. When the incident light was polarized parallel to the slit length, the highest transmittance occurred at shorter wavelengths. The opposite effect was observed for light polarized perpendicular to the slit length, where high transmittance occurred at longer wavelengths, and significant absorption took place at shorter wavelengths. This is different to the behavior of wire-grid polarizers at infrared wavelengths, and is most likely the result of surface plasmon resonance and extraordinary diffraction. In addition to allowing simple device fabrication, the use of an aluminum film enables excitation of surface plasmons in the visible region due to its high plasma frequency.

■KEYWORDS■ Aluminum, Color Filter, Polarization Dependent, Polarization Independent, Surface Plasmon

1. Introduction

Since it was first reported that enhanced optical transmission could occur in metamaterials consisting of optically-thick metallic films with sub-wavelength holes or slits, there has been a great deal of interest in the interaction of light with surface plasmons.⁽¹⁻⁴⁾ Such metamaterials have a wide range of potential applications, including wavelength filters, light extraction from light emitting diodes, and sub-wavelength photolithography.

A particular goal of the present research is the development of optical sensors for use in automotive applications, where high reliability and durability are required. In this regard, metallic color filters are superior to dye filters. Such metallic filters can be realized by exploiting extraordinary optical transmission through periodic sub-wavelength apertures in metal films. This

phenomenon has already been reported for periodic hole arrays in gold and silver films.⁽¹⁻⁴⁾ Our research has focused on aluminum (Al), since in addition to being lower in cost and easier to process, it exhibits lower optical losses at wavelengths of 400 to 500 nm, because its plasma frequency is higher than that of gold or silver. The latter consideration makes Al particularly suitable for blue optical filters, and in fact, we have already demonstrated an Al-based red-green-blue (RGB) color filter.⁽⁵⁻⁸⁾

In many types of applications, filters whose transmittance depends on the polarization of the incident light are commonly used. It should also be possible to fabricate such polarizing filters using metal films containing slit patterns. It has been theoretically predicted that Fano-type interference should occur in thin metal films containing nanoslits,⁽⁹⁻¹²⁾ and this has in fact been confirmed at red wavelengths for a

nanoslit array in a silver film.⁽¹³⁾ However, there has been no experimental validation of such an effect in the blue region. Since this would be necessary in order to realize a broad-spectrum polarizing filter, the present study also considered the effects of a nanoslit array in an Al film on the transmittance of light with different polarizations.

Both hole and slit patterns were fabricated in Al films, and their optical properties were experimentally evaluated. The results were compared with those obtained from calculations using the finite difference time domain (FDTD) method.

2. Light Transmission through Hole and Slit Arrays

2.1 Hole Arrays

When light passed through a hole in a metal, it can couple with guided modes or surface-plasmon (SP) modes on the metal surface, as shown in **Fig. 1**. For guided modes, the light energy is confined within the space between the metal walls, and wavelengths longer than a certain cutoff wavelength are not transmitted through the hole. For the case when the metal is a perfect conductor and the hole is a vacuum, this cutoff wavelength corresponds to half the hole width. In contrast, since SPs represent electron oscillations, and can pass along the inner wall under resonance conditions, light coupled to SPs can propagate through the hole, even if the wavelength is longer than the cutoff wavelength.⁽¹⁻⁴⁾

Based on this concept, the transmittance spectra for hole arrays in Al films were calculated using the FDTD method. The model used for the calculation is shown in **Fig. 2**. It considers an Al film containing a hexagonal lattice of circular holes with a diameter d , and a unit

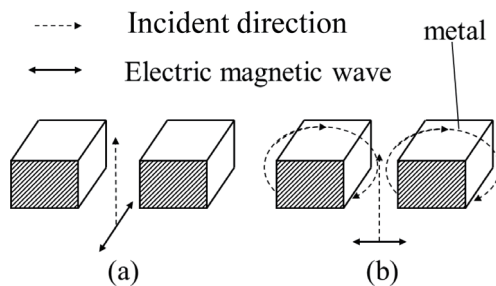


Fig. 1 Diagrammatic representation of the processes responsible for the behavior of the transmission properties. (a) Perfect conductor model. (b) SP mode.

cell spacing of $a=2d$, covered by a passivating SiO_2 layer. **Figure 3** shows the calculated transmittance spectra for hole diameters of 210, 170 and 150 nm, which yield strong transmission in the red, blue and green regions, respectively. The spectra are calculated for the two different polarization angles shown in the inset. It can be seen that transmission occurs at wavelengths greater than twice the hole diameter, and that there is almost no dependence on the polarization direction.

In the spectrum for the red filter in Fig. 3, more than one peak is observed. To investigate the origin of the additional peaks, calculations were performed for different ratios of the hole radius to the lattice constant, and the results are shown in **Fig. 4**. When the r/a ratio is 0.4, three clearly separated peaks at 434, 580 and 657 nm are observed in Fig. 4(a). For these peak wavelengths, the light intensity distributions in the holes at the quartz substrate surface were calculated, and are shown in Figs. 4(b), 4(c) and 4(d), respectively. Since in Fig. 4(d), the light intensity is largest at the hole edge, it can be assumed that this corresponds to an SP mode. In contrast, since most of the light intensity is near the center of the hole in Fig. 4(c), the fundamental guided mode can be

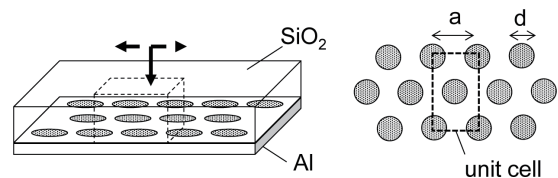


Fig. 2 Numerical calculation model of Al color filter with hole-array.

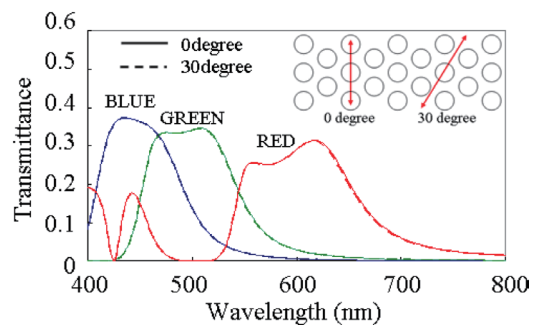


Fig. 3 Polarization dependence of the transmission spectra of aluminum color filters with circular holes (calculated result).

assumed.⁽¹⁸⁾ Finally, the intensity distribution in Fig. 4(b) is thought to be associated with the second guided mode. As can be seen in Fig. 4(a), as the r/a ratio is varied, the position of each peak changes, as indicated by the dashed lines. It is considered that the longest-wavelength peak is the result of the SP mode and the second-longest-wavelength peak is the result of the fundamental guided mode.

2.2 Nanoslit Array

Similar FDTD calculations were carried out using the Al nanoslit model shown in Fig. 5, and the resulting transmittance spectra are shown in Fig. 6 for two

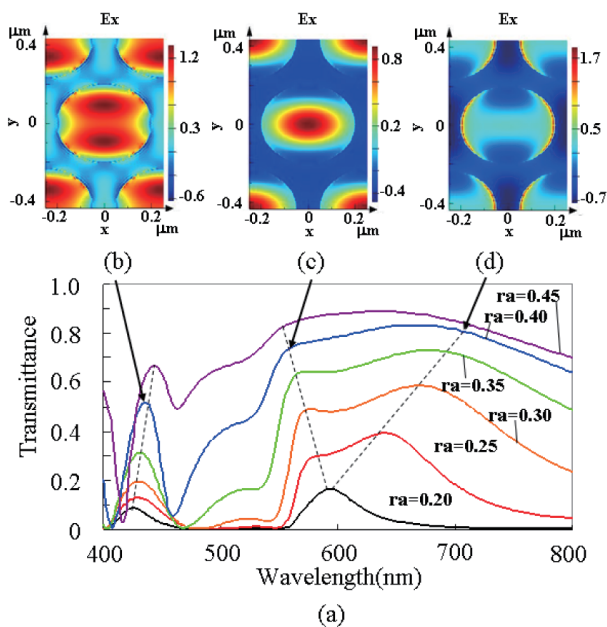


Fig. 4 (a) Transmission spectra of aluminum color filters with circular holes arranged on a hexagonal lattice (calculation result). Intensity profiles of light at (b) 434 nm, (c) 580 nm and (d) 657 nm, respectively.

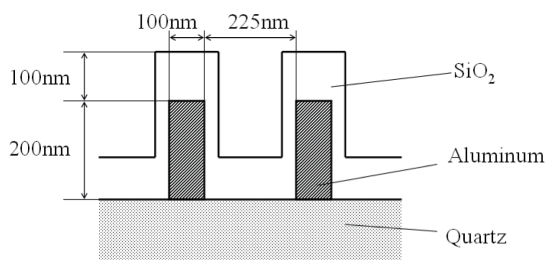


Fig. 5 Cross-sectional view of aluminum filter with nanoslits.

different polarizations. The direction parallel to the slit length is defined as 0° , and corresponds to the TE mode. The direction perpendicular to the slit length is defined as 90° , and corresponds to the TM mode. From Fig. 6, it can be seen that for the TE mode, high transmittance occurs at wavelengths of less than 500 nm. In contrast, for the TM mode, high transmittance occurs above 600 nm, and two strong absorption dips appear at 420 and 480 nm. This differs from the behavior reported for wire-grid polarizers.⁽¹⁴⁾ Whereas the TM mode was strongly transmitted at all wavelengths, the TE mode was preferentially transmitted at shorter wavelengths, and only a single dip was found at longer wavelengths.

For the nanoslit array, the effect of the polarization on the transmittance can be understood by considering the fundamental guided mode^(15,16) and SP modes, as illustrated in Fig. 1. The TE mode cannot couple with an SP mode because the electric field of an SP mode must be perpendicular to the metal surface. Consequently, TM-mode transmission must occur by coupling with a guided mode. This hypothesis was tested by calculating the electric field distribution for the TE and TM modes at 420, 460 and 700 nm. Figures 7(a), 7(b) and 7(c) show the results for the TE mode. In each case, the electric field intensity is strongest at the center of the slit, indicating coupling with the fundamental guided mode. This explains the cutoff that occurs at long wavelengths.

Figures 7(d), 7(e) and 7(f) show the results for the TM mode. In Fig. 7(d) and 7(e), the intensity is strong at the metal side surfaces, indicating coupling

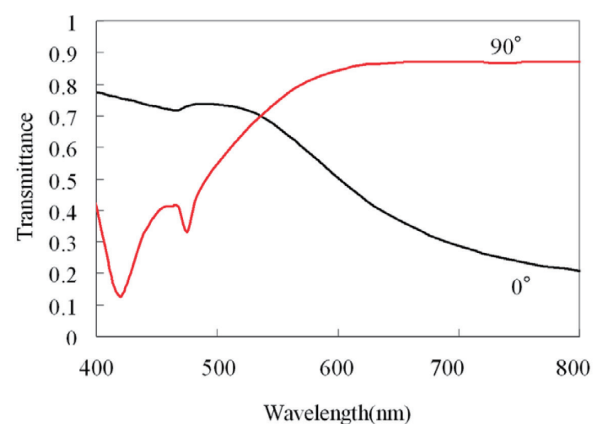


Fig. 6 Polarization dependence of the transmission spectra of aluminum filters with nanoslits. The widths of the slits is 225 nm. (calculated result).

with an SP mode. A dip in the transmission spectrum of the TM mode is observed at 420 nm, which is not observed in the case of wire-grid arrays in the infrared region.⁽¹³⁾ It is considered that this dip is associated with absorption due to a unique SP resonance, and has a different origin to the dip at 460 nm. **Figure 8** shows calculated transmittance spectra for Al slits with various thicknesses of SiO₂. It can be seen that whereas the dip at 420 nm shifts to lower wavelength as the SiO₂ thickness decreases, the dip at 460 nm does not. In addition, although an SP mode can be seen inside the gap in Fig. 7(d) at 420 nm, this is not the

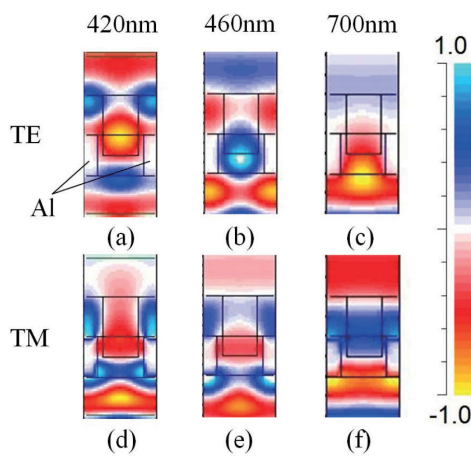


Fig. 7 Electric field profiles of the TE mode at wavelengths of (a) 420 nm, (b) 460 nm, and (c) 700 nm, and those of the TM mode at wavelengths of (d) 420 nm, (e) 460 nm, and (f) 700 nm (calculated result).

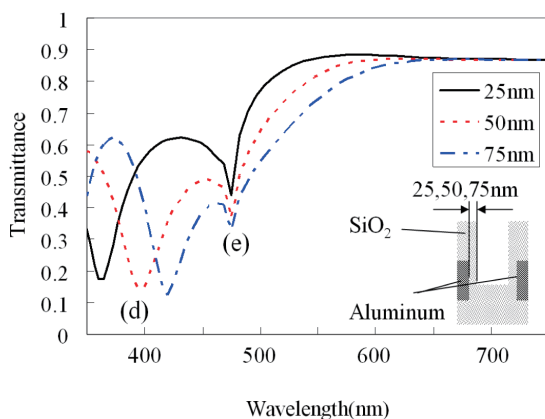


Fig. 8 Transmission spectra of the TM mode for aluminum slits with three different thicknesses of SiO₂. The solid curve is for a thickness of 25 nm; the dashed curve for 50 nm; the dashed-dotted line for 75 nm. (d) corresponds to Fig. 7(d). (e) corresponds to Fig. 7(e).

case in Fig. 7(e) at 460 nm. These results suggest that the dip at 420 nm is due to an SP resonance that travels around the Al metal lines, whereas that at 460 nm is associated with anomalous diffraction determined by the periodicity of the line-and-space pattern.

The existence of both a direct guided mode and a pathway associated with coupled SP resonance and anomalous diffraction, leads to Fano-type interference.⁽⁹⁾

3. Experimental Procedure

3.1 Fabrication Process

The following procedure was used to fabricate the Al nanohole arrays in the present study. A 150-nm-thick Al film was first formed by evaporation on a quartz substrate. A 100-nm-thick SiO₂ film was then deposited using plasma chemical vapor deposition (PD-220NL, SAMCO). An electron beam lithography system (ELS-7000, ELIONIX) was used to expose a 600 $\mu\text{m} \times 600 \mu\text{m}$ region of the SiO₂, and a resist pattern was formed by reactive ion etching (RIE-200NL, SAMCO) with CHF₃. The SiO₂ pattern was then used as a mask to etch a hole-array pattern in the Al film by reactive ion etching (RIE-100iPH, SAMCO) with Cl₂. The resist mask was removed by O₂ plasma ashing. A uniform SiO₂ film was subsequently deposited on the sidewalls of the holes. This is because SP coupling is most efficient when the SP mode frequencies and dielectric constants are the same on opposite sides of the holes. Circular, square and triangular holes were fabricated in square and hexagonal lattice arrangements. The diameter of the circular holes, and the side lengths of the rectangular and triangular holes, was varied from 100 to 350 nm, and the lattice periodicity was always twice this value. **Figure 9** shows plan-view scanning electron

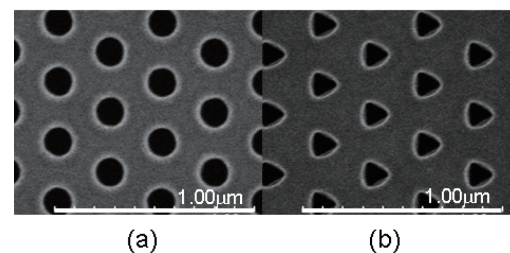


Fig. 9 SEM image of aluminum color filter with (a) circular holes (b) triangular shaped holes.

microscopy (SEM) images of circular and triangular holes.

A similar fabrication process was used for the Al nanoslits. Figure 5 shows a schematic of the nanoslit structure. Again, a final SiO₂ film was deposited in order to match the SP modes on either side of the slits and to prevent oxidation. The width, period and height of the slits were 225, 325 and 200 nm, respectively. **Figure 10** shows a plan-view SEM image of the slit array. Because the Al lines had a high aspect ratio and easily fell over, Al crossbeams were used to provide support. The FDTD method was used to determine an appropriate crossbeam spacing in order to avoid detrimental effects on the optical properties, and the final spacing chosen was 5 μm .

3.2 Measurements

To measure the optical transmittance spectra, the samples were placed on the stage of an optical microscope (NIKON, X2F-UNR), and illuminated using a polarized white light source. The transmitted light was sent to a spectrometer (PMA-11, Hamamatsu Photonics) using an optical fiber. The incident and transmitted beam directions were along the sample surface normal.

4. Results and Discussion

4.1 Hole Arrays

Figure 11 shows transmission optical micrographs for the four different hole patterns shown in the SEM images in the insets. The scale on the right-hand side shows the lattice periodicity. Since the incident

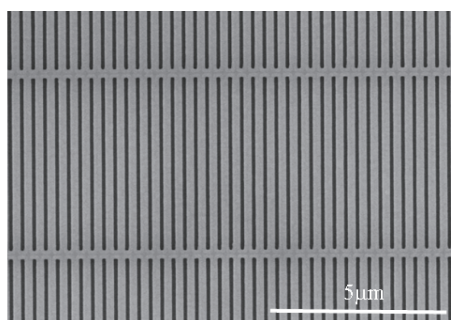


Fig. 10 SEM image of aluminum filter with nanoslits.

illumination is white light, it is clear from this figure that effective color filtering can be achieved.

Figure 12 shows an optical micrograph obtained using a filter containing patterned regions of triangular holes with sides of 210, 170 and 150 nm for red, green and blue, respectively. Despite the fact that the side lengths are shorter than the wavelength of the visible light, the light has successfully penetrated the Al film. A blue color can be observed over an area of 150 $\mu\text{m} \times 150 \mu\text{m}$.

Transmittance spectra for RGB color filters with

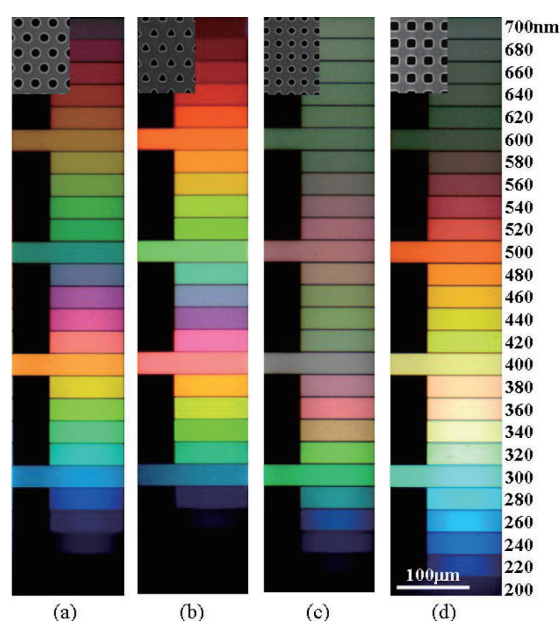


Fig. 11 Optical microscope images of aluminum color filters with (a) circular holes arranged on a hexagonal lattice, (b) triangular shaped holes, (c) circular holes arranged on a square lattice, and (d) square holes. The numbers beside the photographs give the period of the arrays in nanometer.

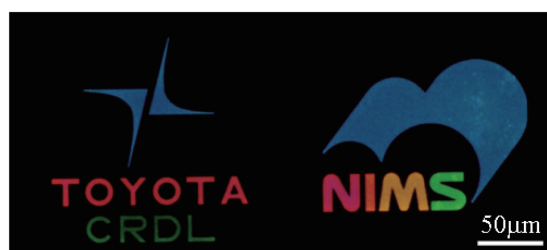


Fig. 12 Optical microscope image of aluminum color filter with triangular shaped holes.

triangular and circular holes are shown in **Fig. 13**. It can be seen that, although higher transmittance is achieved with the circular holes, the bands are more narrow for the triangular holes. Since a narrower bandwidth is considered to be more important, the filter with the triangular holes is superior.

Figure 14 shows the polarization dependence of the transmittance spectra for filters with circular holes with a diameter of 210, 170 and 150 nm in a hexagonal lattice. The solid and dashed lines indicate a polarization of 0° and 30°, respectively. It can clearly be seen that there is no dependence on the polarization angle, which is consistent with the calculation results shown in Fig. 3.

4.2 Nanoslits

Figure 15 shows optical micrographs of light transmitted through the filter with the slit pattern in

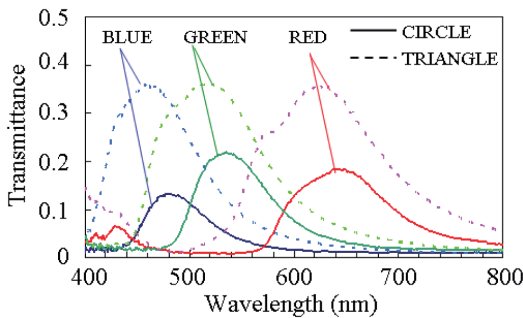


Fig. 13 Transmission spectra of RGB color filters with triangular holes (solid line) and round holes (solid line).

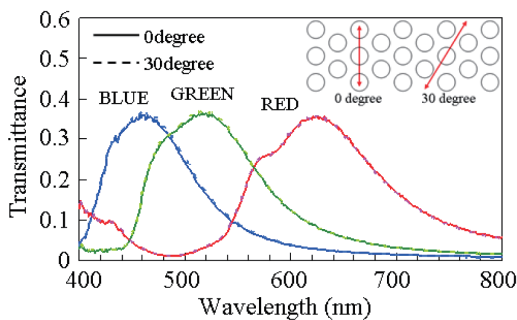


Fig. 14 Polarization dependence of transmission spectra of RGB color filters with circular holes (experimental result).

Fig. 5. The filter is illuminated with white light with different polarization angles, and the color of the transmitted light clearly varies with polarization angle. For a polarization of 0° (TE mode), it appears blue, whereas for a polarization of 90° (TM mode), it appears orange.

Figure 16 shows transmittance spectra for this filter for different polarization angles. At long wavelengths, the filter behaves in a similar manner to a wire-grid array, in that the TE mode is absorbed, but the TM mode is not. However, different behavior is seen in the short wavelength region. For the TM mode, two dips appear at 420 and 460 nm, which is consistent with the calculation results shown in Fig. 6. Thus, the nanoslit array acts as a low-pass filter for the TE mode, and a

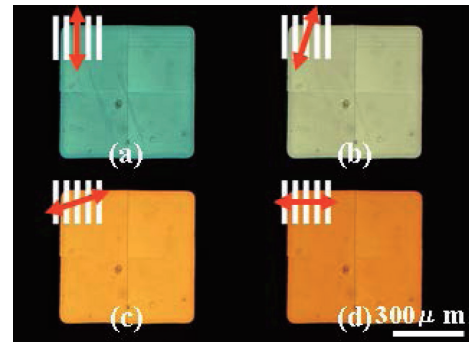


Fig. 15 Optical microscope images of aluminum filters with nanoslits. The width of the slits is 225 nm. The direction of polarization in (a) is parallel to the slits (we define this angle as 0°). The direction of polarization in (b) is tilted at 30°, in (c) at 60°, and in (d) at 90°.

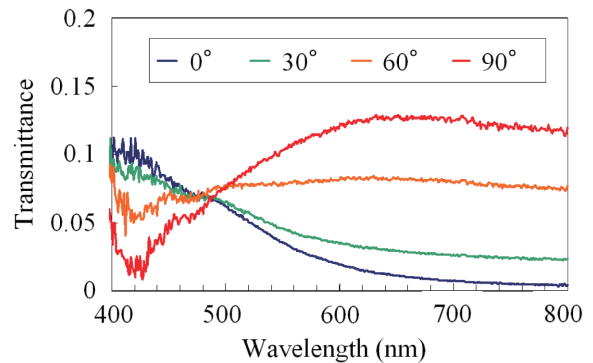


Fig. 16 Polarization dependence of the transmission spectra of aluminum filters with nanoslits. The width of the slits is 225 nm. (experimental result).

high-pass filter for the TM mode.

Although there is generally good qualitative agreement between the experimental and calculation results, the experimental transmittance is generally lower. This is considered to be due to the surface roughness on the SiO₂ passivation layer. The SP and guided modes are both sensitive to such roughness, which causes scattering and reduces the transmittance.

5. Summary

The optical properties of arrays of nanoholes and nanoslits in Al films were investigated both numerically and experimentally. The choice of Al was based on its low cost and ease of processing, in addition to the fact that it has a higher plasma frequency than gold or silver, leading to lower optical losses at wavelengths of 400 to 500 nm. For a hexagonal array of circular holes, the transmittance was found to be independent of the polarization of the incident light. By suitable choice of hole size and lattice periodicity, the arrays could be made to act as filters over the entire visible region. In the blue region, the effects of SP mode coupling and extraordinary diffraction were clearly evident. For the nanoslit filter, the transmittance was strongly dependent on the polarization of the incident light, and it acted as a low-pass filter for the TE mode, and a high-pass filter for the TM mode. This behavior was explained in terms of Fano-type interference.

References

- (1) Ebbesen, T. W., Lezec, H. J., Ghaemi, H. F., Thio, T. and Wolff, P. A., "Extraordinary Optical Transmission through Sub-wavelength Hole Arrays", *Nature*, Vol. 391 (1998), pp. 667-669.
- (2) Barnes, W. L., Dereux, A. and Ebbesen T. W., "Surface Plasmon Subwavelength Optics", *Nature*, Vol. 424 (2003), pp. 824-830.
- (3) Genet, C. and Ebbesen T. W., "Light in Tiny Holes," *Nature*, Vol. 445 (2007), pp. 39-46.
- (4) Krishnan, A., Thio, T., Kim, T. J., Lezec, H. J., Ebbesen, T. W., Wolff, P. A., Pendry, J., Martín-Moreno, L. and García-Vidal, F. J., "Evanescently Coupled Resonance in Surface Plasmon Enhanced Transmission", *Optics Commun.*, Vol. 200, No. 1-6 (2001), pp. 1-7.
- (5) Ikeda, N., Tsuya, D., Sugimoto, Y., Koide, Y., Asakawa, K., Miura, A., Inoue, D., Nomura, T., Fujikawa, H. and Sato, K., *Proc. of Int. Symp. on Photonic and Electromagnetic Crystal Structures Meeting VIII*, (2009), PECS.
- (6) Inoue, D., Nomura, T., Miura, A., Fujikawa, H., Sato, K., Ikeda, N., Tsuya, D., Sugimoto, Y., Koide, Y. and Asakawa, K., "RGB Color Filter Comprising Aluminum Film with Surface Plasmon Enhanced Transmission through Sub-wavelength Hole-arrays", *Proc. IEEE Conf. on Optical MEMS & Nanophotonics*, (2009), pp. 150-151, IEEE.
- (7) Inoue, D., Nomura, T., Miura, A., Fujikawa, H., Sato, K., Ikeda, N., Tsuya, D., Sugimoto, Y., Koide, Y. and Asakawa, K., "Polarization Independent RGB Color Filter Comprising an Aluminum Film with Surface Plasmon Enhanced Transmission through a Sub-wavelength Array of Holes", *Appl. Phys. Lett.*, Vol. 98, No. 9 (2011), 093113.
- (8) Inoue, D., Nomura, T., Miura, A., Fujikawa, H., Sato, K., Ikeda, N., Tsuya, D., Sugimoto, Y. and Koide, Y., "Polarization Filters for Visible Light Consisting of Sub-wavelength Slits in an Aluminum Film", *J. of Lightwave Technology*, Vol. 30, No. 22 (2012), pp. 3463-3467.
- (9) Sarrazin, M., Vigneron, J.-P. and Vioureaux, J.-M., "Role of Wood Anomalies in Optical Properties of Thin Metallic Films with a Bidimensional Array of Subwavelength Holes", *Phys. Rev. B*, Vol. 67 (2003), 085415.
- (10) Catrysse, P. B. and Fan, S., "Nanopatterned Metallic Films for Use as Transparent Conductive Electrodes in Optoelectronic Devices", *Nano Lett.*, Vol. 10, No. 8 (2010), pp. 2944-2949.
- (11) Wood, R. W., "On a Remarkable Case of Uneven Distribution of Light in a Diffraction Grating Spectrum", *Proc. of the Phys. Soc. of London*, Vol. 18 (1902), pp. 269-275.
- (12) Fano, U., "Effects of Configuration Interaction on Intensities and Phase Shifts", *Phys. Rev.*, Vol. 124, No. 6 (1961), pp. 1866-1878.
- (13) Jug, Y. S., Sun, Z., Wuenschell, J. and Kim, H. K., "High-sensitivity Surface Plasmon Resonance Spectroscopy Based on a Metal Nanoslit Array", *Appl. Phys. Lett.*, Vol. 88 (2006), 243105.
- (14) Xu, M., Urbach, H. P., De Boer, D. K. G and Cornelissen, H. J., "Wire-grid Diffraction Gratings Used as Polarizing Beam Splitter for Visible Light and Applied in Liquid Crystal on Silicon", *Opt. Exp.*, Vol. 13, No. 7 (2005), pp. 2303-2320.
- (15) Catrysse, P. B. and Fan, S., "Near-complete Transmission through Subwavelength Hole Arrays in Phonon-polaritonic Thin Films", *Phys. Rev. B*, Vol. 75, No. 7 (2007), 075422.
- (16) Rodrigo, S. G., García-Vidal, F. J. and Martín-Moreno, L., "Influence of Material Properties on Extraordinary Optical Transmission through Hole Arrays", *Phys. Rev. B*, Vol. 77 (2008), 075401.
- (17) Vial, A. and Laroche, T., "Comparison of Gold and Silver Dispersion Laws Suitable for FDTD Simulations", *Appl. Phys. B*, Vol. 93, No. 1 (2008), pp. 139-143.

Figs. 1, 5-8, 10, 15 and 16

Reprinted from J. of Lightwave Technology, Vol. 30, No. 22 (2012), pp. 3463-3467, Inoue, D., Nomura, T., Miura, A., Fujikawa, H., Sato, K., Ikeda, N., Tsuya, D., Sugimoto, Y. and Koide, Y., "Polarization Filters for Visible Light Consisting of Subwavelength Slits in an Aluminum Film", © 2012 IEEE, with permission from IEEE.

Figs. 3, 4, 9 and 11-14

Reprinted from Appl. Phys. Lett., Vol. 98, No. 9 (2011), 093113, Inoue, D., Miura, A., Nomura, T., Fujikawa, H., Sato, K., Ikeda, N., Tsuya, D., Sugimoto, Y. and Koide, Y. "Polarization Independent Visible Color Filter Comprising an Aluminum Film with Surface-plasmon Enhanced Transmission through a Subwavelength Array of Holes", © 2011 AIP, with permission from AIP.

Daisuke Inoue

Research Fields:

- LIDAR (Laser Imaging Detection and Ranging)
- Optical Integrated Circuit

Academic Degree: Dr.Eng.

Academic Society:

- IEEE



Atsushi Miura

Research Field:

- Nano Fabrication-processes for Photonic Devices

Academic Society:

- IEEE

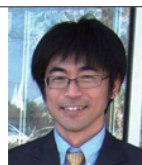


Tsuyoshi Nomura

Research Fields:

- Numerical Analysis of Composite Materials
- Topology Optimization

Academic Degree: Dr. Eng.



Hisayoshi Fujikawa

Research Fields:

- Organic Light-emitting-diode
- Plasmonic Devices

Academic Degree: Dr.Eng.

Academic Societies:

- The Japan Society of Applied Physics
- The Optical Society of Japan



Kazuo Sato

Research Fields:

- Antennas for Mobile Communication
- Automotive Radar

Academic Degree: Dr.Eng.

Academic Societies:

- IEEE
- The Institute of Electronics, Information and Communication Engineers



Naoki Ikeda*

Research Field:

- Nanoprocessing Technologies for Nanophotonic Devices such as Photonic Devices

Academic Degree: Dr.Eng.

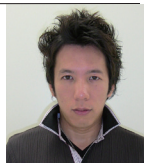


Daiju Tsuya*

Research Field:

- Nano/Microfabrication Technology for Advanced Nanomaterials

Academic Degree: Dr.Eng.



Yoshimasa Sugimoto*

Research Fields:

- Nanoprocessing Technologies for Nanophotonic Devices such as Photonic Crystals for Ultra-fast Photonic Devices
- Plasmonic Optical Color Filters and Metamaterial Devices

Academic Degree: Ph.D



Yasuo Koide*

Research Field:

- Electrical and Optical Device Properties of Diamond

Academic Degree: Ph.D



*National Institute for Materials Science (NIMS)